Latitudinal dependence of Atlantic meridional overturning circulation (AMOC) variations

Rong Zhang[1]

Received 24 June 2010; accepted 6 July 2010; published 21 August 2010.

[1] AMOC variations are often thought to propagate with the Kelvin wave speed, resulting in a short time lead between high and low latitudes AMOC variations. However as shown in this paper using a coupled climate model (GFDL CM2.1), with the existence of interior pathways of North Atlantic Deep Water (NADW) from Flemish Cap to Cape Hatteras as that observed recently, AMOC variations estimated in density space propagate with the advection speed in this region, resulting in a much longer time lead (several years) between subpolar and subtropical AMOC variations and providing a more useful predictability. The results suggest that AMOC variations have significant meridional coherence in density space, and monitoring AMOC variations in density space at higher latitudes might reveal a stronger signal with a several-year time lead. **Citation:** Zhang, R. (2010), Latitudinal dependence of Atlantic meridional overturning circulation (AMOC) variations, *Geophys. Res. Lett.*, *37*, L16703, doi:10.1029/2010GL044474.

1. Introduction

[2] The AMOC variability is often thought to be a major source of multidecadal climate variations [*Delworth and Mann*, 2000; *Knight et al.*, 2005; *Zhang*, 2008]. Changes in the anthropogenic forcing due to increasing greenhouse gases might lead to a slowdown of AMOC in the 21st century [*Schmittner et al.*, 2005]. The pioneering RAPID program was established recently to monitor AMOC variations at 26.5°N [*Cunningham et al.*, 2007]. However, the latitudinal dependence and propagation of AMOC variations remains unclear. This paper studies the latitudinal dependence and propagation of AMOC variations using a fully coupled model (GFDL CM2.1 [*Delworth et al.*, 2006]).

[3] The AMOC is often estimated in depth space which shows a maximum south of the subpolar region (Figure S1 of the auxiliary material).[2] In density space (Figure 1a), the maximum AMOC (25.7 Sv, $1Sv = 10^6$ m^3 s^{-1}) is shifted to the subpolar region, similar to estimates using the observed hydrographic data [*Talley et al.*, 2003]. North of 45°N, the steep isopycnals below 200m are almost perpendicular to the isobars (Figure 1b). The strong gradient of the overturning stream function across a very narrow density range around 1036.8 kg/m^3 (Figure 1a) corresponds to the southward deep flow of NADW moving along these isopycnals that are very steep north of 45°N. The strong vertical recirculation south of NADW formation sites (Figure 1a) generates a maximum AMOC there. In depth space north of 45°N, the northward and southward transports compensate each other within the same depth layer, disguising the maximum AMOC near NADW formation sites and resulting in a maximum at lower latitudes (Figure S1). Hence the typical estimation of AMOC in depth space is not suitable at mid and high latitudes. For studies of subpolar AMOC variations or their meridional connectivity with those in the subtropics, AMOC variations need to be estimated in density space, instead of depth space.

2. Latitudinal Dependence of AMOC Variations in the Control Simulation

[4] The AMOC variability is stronger at middle and high latitudes North Atlantic than that at low latitudes North Atlantic and the South Atlantic (Figures 2a and 2b). The recirculation cell south of NADW formation sites (Figure 1a) is very sensitive to changes in NADW formation and causes stronger variations there. For example, AMOC variations at 49.5°N lag Labrador Sea mixed layer depth variations by 2 years with a significant correlation of 0.6. North of 40°N, the AMOC variability in depth space starts to diverge from that in density space and weakens significantly (Figure 2b), thus can not represent the real AMOC variability.

[5] The southward propagation of AMOC variations associated with changes in NADW formation can be classified into three regimes in the Atlantic (Figure 2c) due to different mechanisms. In regime I (mid to high latitude North Atlantic), AMOC variations propagate with the advection speed, and there is a 4-year lead between AMOC variations at 50°N and at 34°N. A large fraction of the NADW outflow moves away from the western boundary and enters into the interior ocean near Flemish Cap and the Grand Banks (Figure S2), consistent with interior pathways observed recently [*Bower et al.*, 2009]. The advective time scale (T_{adv}) is estimated by the equation $T_{adv} = L/V$, where L (about 1780 km) is the meridional distance between 50°N and 34°N, and V (about 1.5 cm/s) is the modeled climatological mean meridional velocity of the NADW outflow along interior pathways from 50°N to 34°N averaged over the 1800m to 4000m depth range from the control simulation, which gives an advective time scale of about 3.8 years. This is consistent with the observation that it takes about 6 years for the Labrador Sea Water thickness anomaly signal to reach the subtropics [*Curry et al.*, 1998]. (Note that the Labrador Sea mixed layer depth variations lead the AMOC variations at 49.5°N by about 2 years.) The advection speed is also consistent with the CFC tracer based estimates [*Smethie*, 1992].

[6] In regime II (from south of 34°N to the equator), both upper and deep meridional flows move mainly along the

[1]GFDL, NOAA, Princeton, New Jersey, USA.

[1]Auxiliary materials are available in the HTML. doi:10.1029/2010GL044474.

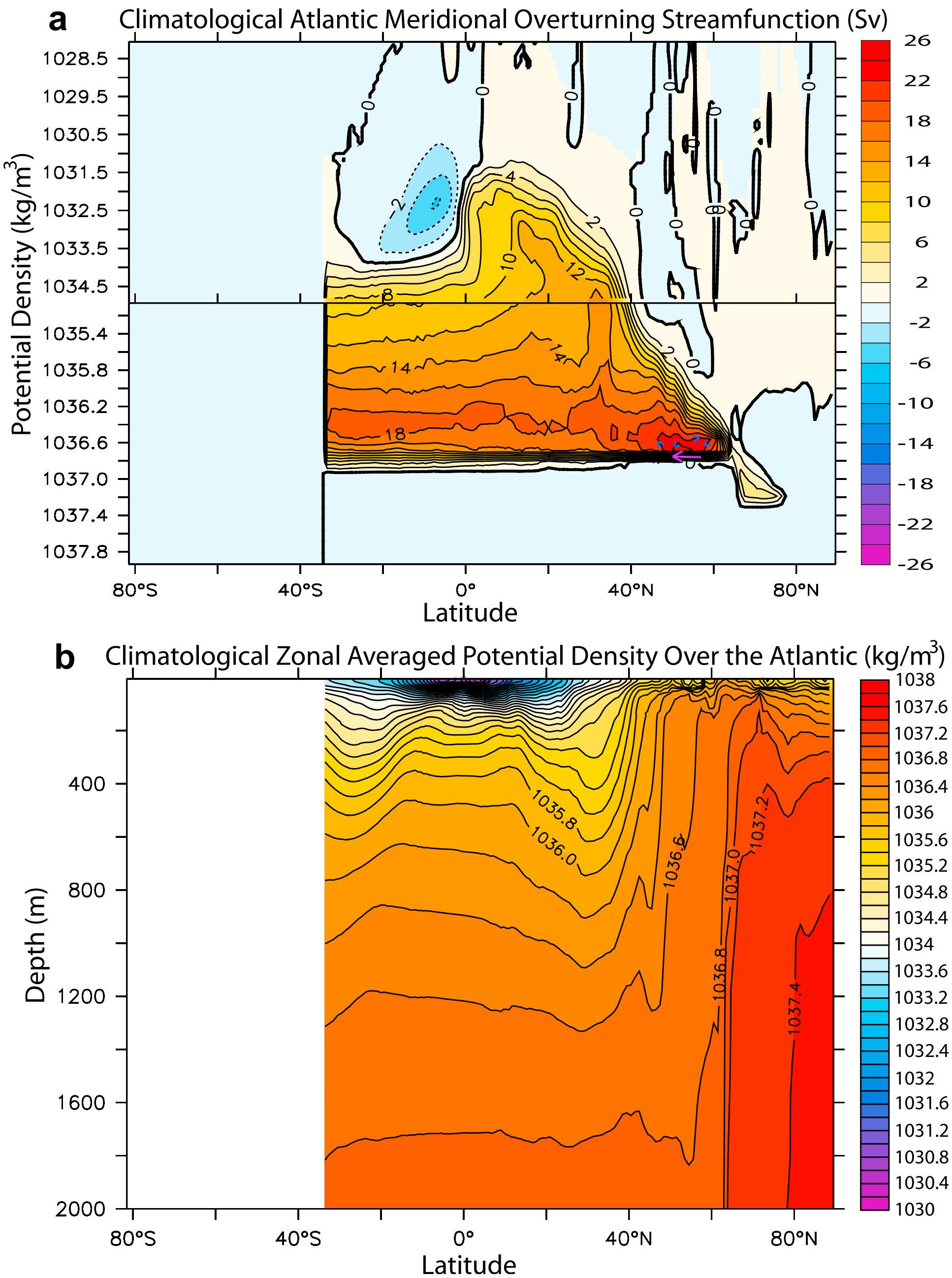

Figure 1. (a) Climatological annual mean zonal integrated meridional overturning streamfunction (Sv) in the Atlantic in potential density (referenced to 2000m) space and (b) climatological annual mean potential density zonal averaged over the Atlantic (kg/m^3) from the GFDL CM2.1 1000-year control simulation.

western boundary, not through interior pathways (Figure S2). Because of no cross-boundary flow condition along the western boundary, the anomalous velocity propagates southward with rapid coastal Kelvin waves [*Kawase*, 1987; *Johnson and Marshall*, 2002]. Hence AMOC variations at various latitudes in Regime II are almost in phase (Figure 2c). The Kelvin waves move quickly eastward at the equator, and poleward along the eastern boundary [*Kawase*, 1987; *Johnson and Marshall*, 2002]. In regime III (South Atlantic), the anomaly signal at the eastern boundary is carried westward by Rossby waves with a slower speed at higher latitudes than at lower latitudes [*Johnson and Marshall*, 2002]. Rossby waves can have some impact in Regime II [*Johnson and Marshall*, 2002] but their main impact is in Regime III due to the absent of Kelvin waves at the western boundary there. It takes about 3 years for the Rossby waves to cross the basin at 34°S, thus AMOC variations at 34°S lags those at the equator by about 3 years (Figure 2c).

[7] The earlier study of the propagation of AMOC variations [*Kawase*, 1987; *Johnson and Marshall*, 2002; *Getzlaff et al.*, 2005] is within the framework of the Kelvin wave response based on the classic picture that the NADW outflow moves along the western boundary as DWBC, without considering the impact of newly observed interior pathways. The paper here is focused on the fundamental question: Given a partial detachment of the DWBC and the interior pathways of

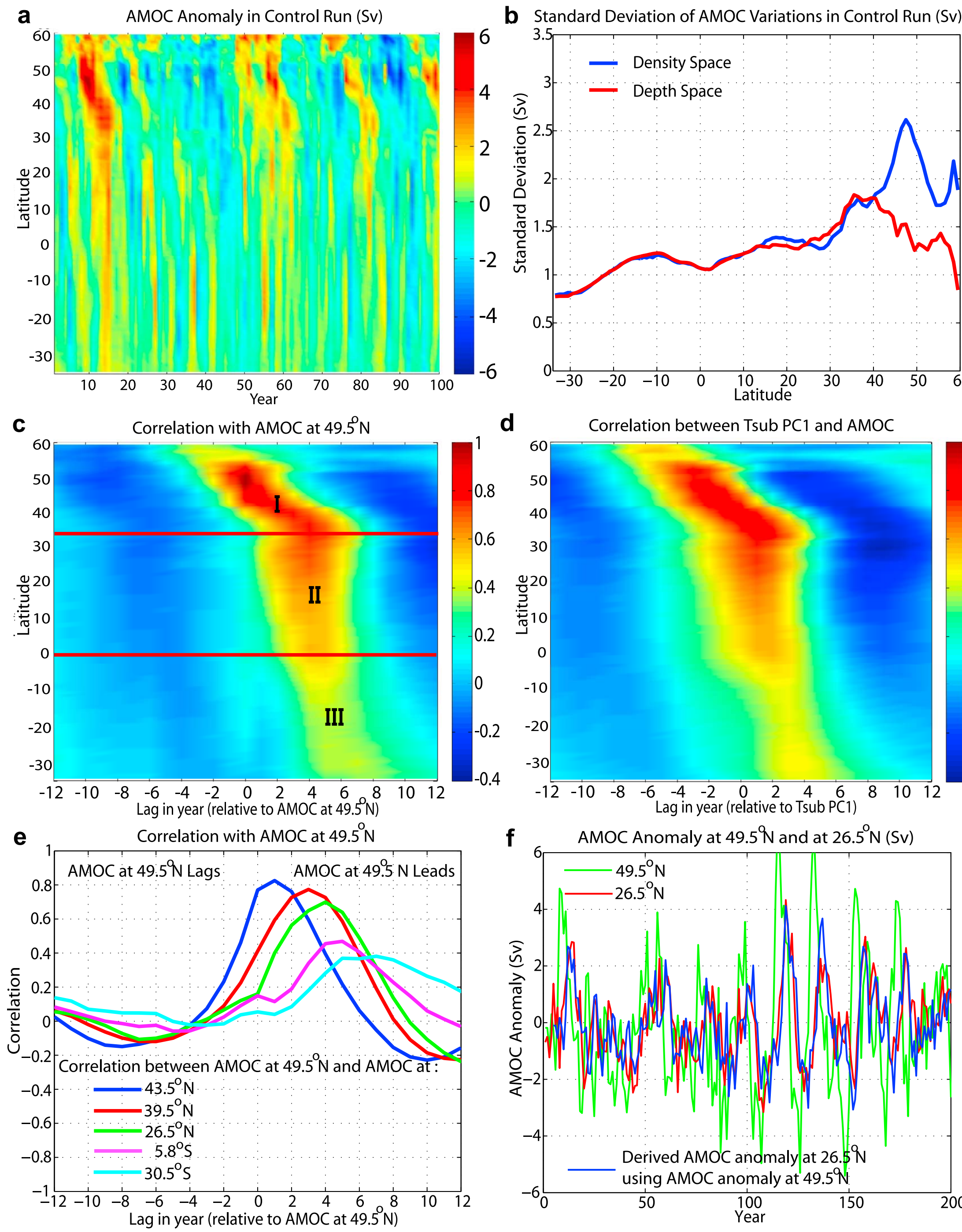

Figure 2. AMOC variations in the 1000-year control simulation. The AMOC Index at each latitude is defined as the maximum of the annual mean zonal integrated Atlantic overturning streamfunction in **Density** space, except in Figure 2b AMOC is estimated in both density and depth space for comparison. (a) AMOC anomaly vs. latitudes for the first 100 years. (b) Standard deviation of AMOC variations vs. latitudes. (c) Correlation between AMOC variations at 49.5°N and AMOC variations at all latitudes over the entire control simulation. The horizontal red lines mark boundaries of the three regimes (I, II, III) of the southward propagation of AMOC variations. (d) Correlation between Tsub PC1 and AMOC variations at all latitudes. (e) Correlation between AMOC variations at 49.5°N and AMOC variations at 43.5°N, 39.5°N, 26.5°N, 5.8°S, and 30.5°S respectively. (f) AMOC anomaly at 49.5°N (green) and at 26.5°N (red) for the first 200 years in control simulation, and the derived AMOC anomaly at 26.5°N by taking a 4-year lag of AMOC anomaly at 49.5°N and multiplying it with the ratio of standard deviations of AMOC variations between the two latitudes.

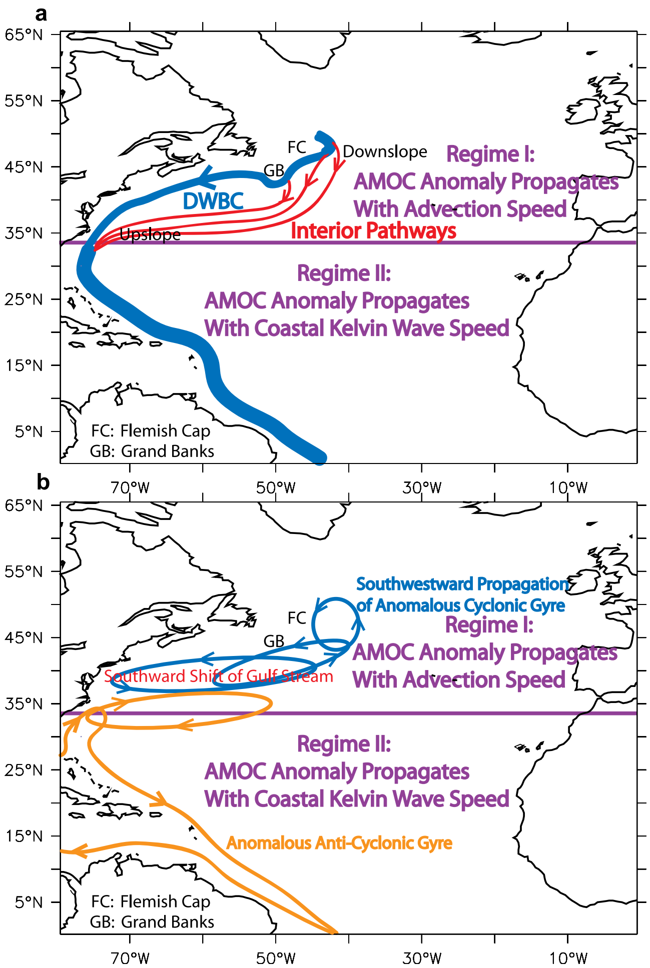

Figure 3. (a) Schematic diagram of the propagation of a positive AMOC anomaly induced by enhanced NADW formation. In Regime II, there are no interior pathways. (b) The AMOC anomaly propagates with Kelvin wave speed, inducing an anti-cyclonic anomalous barotropic gyre (orange, Figure 3b). In Regime I, part of the DWBC moves downslope around Flemish Cap as well as the Grand banks, thus is partially detached from the western boundary and moves along interior pathways as observed (Figure 3a). Hence the AMOC anomaly propagates with the second stage advection speed. The initial stage is the same as in Regime II; in the second stage, some anomalous deep flow moves downslope along interior pathways with advection speed, interacts with bottom topography to induce an anomalous cyclonic gyre (blue, Figure 3b) propagating southwestward with advection speed, strengthening the DWBC and pushing the Gulf Stream path southward. Around 35°N, the anomalous interior deep flow moves upslope to rejoin the DWBC, inducing an anomalous anti-cyclonic gyre (orange, Figure 3b) and reinforcing the anomaly in Regime II.

NADW outflow in Regime I, will AMOC variations still propagate with the Kelvin wave speed? This paper found that the existence of interior pathways of NADW outflow in Regime I causes a fundamentally different propagation mechanism (auxiliary material and Figure 3), resulting in a several-year time lead between subpolar and subtropical AMOC variations.

[8] In Regime I, the propagation of a positive AMOC anomaly is in two stages. The initial stage is the Kelvin wave response with an anomalous anti-cyclonic barotropic gyre developed along North America east coast, same as that in Regime II (Figures S3a and S3b). In the second stage, the interior deep flow anomaly moves with a similar speed as the density anomaly that is advected by the mean flow along interior pathways, because it can not propagate with the Kelvin wave speed in interior. It interacts with the bottom topography and induces a positive bottom vortex stretching anomaly (downslope), thus an anomalous barotropic cyclonic gyre [*Zhang and Vallis*, 2007]. The anomalous cyclonic gyre propagates southwestward with the interior deep flow anomaly on the same advection time scale (Figure S3), replaces the initial Kelvin wave induced anti-cyclonic gyre, strengths the DWBC, and pushes the Gulf Stream path southward when it propagates to south of the Grand Banks a few years later. Meanwhile an anomalous anti-cyclonic gyre is developed in the subpolar open ocean (Figure S3e) due to the weakened mixed layer depth there. This dipole pattern also presents in modeled and observed leading mode of North Atlantic Subsurface Temperature (Tsub) and is a fingerprint of AMOC variations [*Zhang*, 2008]. The relationship between a stronger AMOC/DWBC and a southward shift of the Gulf Stream has been modeled [*Gerdes and Köberle*, 1995; *Zhang and Vallis*, 2007] and is consistent with the observation from Line W [*Peña-Molino and Joyce*, 2008].

[9] AMOC variations at 49.5°N lag the DWBC anomaly at 53°N by 1 year, but lead the DWBC anomaly at 65°W and the interior southwestward deep flow anomalies at the same latitude (39°N) by 3 years (Figure S4). Hence the DWBC anomaly after the two-stage adjustment varies with the interior deep flow anomaly on the advection time scale, and the AMOC anomaly (includes both interior flow and DWBC anomalies) propagates with the second stage advection speed in Regime I. The same advection time scale can also be seen from the southward propagation of younger age tracer in the deep ocean in Regime I associated with a positive AMOC anomaly (Figure S5).

[10] The AMOC fingerprint (Tsub PC1 [*Zhang*, 2008]) is in phase with AMOC variations around 39.5°N (Figure 2d). The Atlantic Multidecadal Oscillation (AMO), often defined as the Sea Surface Temperature (SST) anomaly averaged over the entire North Atlantic [*Knight et al.*, 2005], is in phase with AMOC variations at 38.5°N. The simulated AMOC anomaly at 49.5°N leads that at 26.5°N by 4 years with a maximum correlation of 0.7 (Figures 2e and 2f), explaining about 49% of the AMOC variance at the low latitudes. At zero time lag the correlation between AMOC variations at the two latitudes is much lower (0.17, Figure 2e). A similar low correlation at zero time lag in depth space is found in the previous study [*Bingham et al.*, 2007] and interpreted as a low meridional coherence between subpolar and subtropical AMOC variations. Here I show that in density space the AMOC variations at high latitudes are significantly connected with those at low latitudes but with a several-year time lead due to the advection time scale.

3. Two-Stage Adjustment to an Abrupt Change at High Latitudes

[11] A previous ocean-only modeling study with prescribed surface fluxes [*Getzlaff et al.*, 2005] shows that the AMOC propagation in depth space is faster in higher resolution models due to the faster Kelvin wave speed. However,

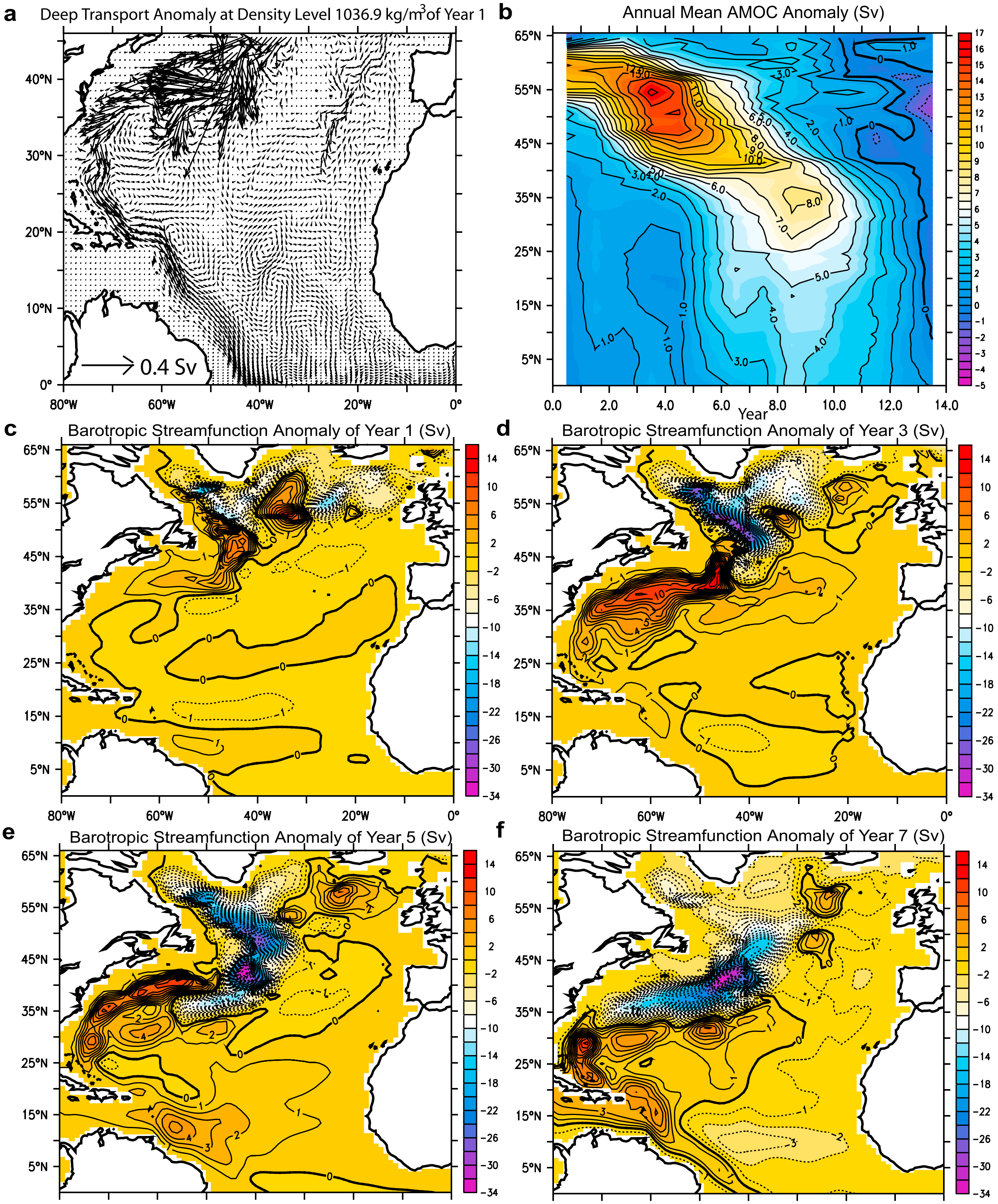

Figure 4. Annual mean anomalies from the ensemble of perturbed experiments. (a) Deep transport anomaly at potential density level 1036.9 kg/m^3 of year 1. (b) Temporal evolution of AMOC anomaly as a function of latitude. (c–f) Barotropic streamfunction anomaly of year 1, 3, 5, 7.

even with the slowdown of Kelvin wave in B-grid 1° coarse resolution model, the Kelvin wave propagation time scale from high to low latitude North Atlantic is on the order of several months, not several years [*Hsieh et al.*, 1983]. To show that the 4-year time lead between subpolar and subtropical AMOC variations found in GFDL CM2.1 is not due to the slowdown of the first stage Kelvin wave speed, but due to the second stage adjustment, an ensemble of 5-member perturbed experiments were conducted for 14 years using GFDL CM2.1 (auxiliary material), with a strong positive salinity anomaly (0.5 PSU) added to the upper northern North Atlantic and the Nordic Sea in the initial ocean condition.

[12] The initial positive salinity perturbation induces an abrupt increase in both the Labrador Sea and the Nordic Sea annual mean mixed layer depth by more than 1000m at year 1. The southward deep transport anomaly triggered by the stronger high latitude deep convection propagates to the equator along the western boundary within 1 year due to the fast first stage Kelvin wave response (Figure 4a). The AMOC anomaly at 49.5°N reaches a maximum at year 4.5, while the AMOC anomaly in Regime II reaches the maximum at year 8.5 (Figure 4b). The 4-year time lag between them is inconsistent with the first stage Kelvin wave adjustment, but due to the slow Second Stage advection adjustment: i.e., the anomalous anti-cyclonic gyre induced by Kelvin waves in Regime I is gradually replaced by an anomalous cyclonic gyre induced by the anomalous interior deep flow and propagating southwestward from the subpolar region to the subtropics on the tracer advection time scale (Figures 4c–4f). When the anomalous cyclonicgyre propagates to south of the Grand Banks, it strengthens the DWBC and pushes the Gulf Stream path southward. Around Cape Hatteras, the anomalous interior deep flow moves upslope to rejoin the DWBC, inducing an anomalous anti-cyclonic gyre there, which reinforces the anomalous anti-cyclonic gyre in Regime II (Figure 4f).

4. Conclusion and Discussion

[13] The modeling results in this paper show that with the existence of interior pathways of the export of NADW from Flemish Cap to Cape Hatteras as that observed recently, AMOC variations in this region propagate with the advection speed, resulting in a much longer time lead (several years) between subpolar and subtropical AMOC variations in the North Atlantic. The longer time lead provides a more useful predictability. The results suggest that monitoring AMOC variations in density space at higher latitudes North Atlantic might reveal a stronger signal that leads AMOC variations at lower latitudes by several years.

[14] One caveat of the study is that the GFDL CM2.1 ocean component lacks explicit eddies, has broaden boundary currents and weaker DWBC from Flemish Cap to Cape Hatteras than that observed, and slows down the Kelvin wave artificially. The results need to be improved in future studies with higher resolution models.

[15] Eddy-resolving simulations [*Smith and Gent*, 2004; *Bower et al.*, 2009] also show that a significant part of NADW outflow moves along interior pathways in Regime I. In eddy-resolving models, the initial first stage Kelvin wave adjustment would be much faster; however, the propagation of AMOC anomaly in Regime I would be affected by the second stage slow advection process due to the existence of interior pathways. The eddy-resolving models might simulate stronger advection speed, but have more horizontal recirculation along interior pathways [*Smith and Gent*, 2004]. The two factors counter each other and the net advection time scale might still be on order of a few years.

[16] **Acknowledgments.** I thank Kirk Brian, Thomas L. Delworth, Salil Mahajan, and two anonymous reviewers for very helpful suggestions.

References

Bingham, R. J., C. W. Hughes, V. Roussenov, and R. G. Williams (2007), Meridional coherence of the North Atlantic meridional overturning circulation, *Geophys. Res. Lett.*, *34*, L23606, doi:10.1029/2007GL031731.
Bower, A. S., M. S. Lozier, S. F. Gary, and C. W. Böning (2009), Interior pathways of the North Atlantic meridional overturning circulation, *Nature*, *459*, 243–248, doi:10.1038/nature07979.
Cunningham, S. A., et al. (2007), Temporal variability of the Atlantic meridional overturning circulation at 26.5°N, *Science*, *317*, 935–938.
Curry, R. G., M. S. McCartney, and T. M. Joyce (1998), Oceanic transport of subpolar climate signals to mid-depth subtropical waters, *Nature*, *391*, 575–577.
Delworth, T. L., and M. E. Mann (2000), Observed and simulated multidecadal variability in the Northern Hemisphere, *Clim. Dyn.*, *16*, 661–676.
Delworth, T. L., et al. (2006), GFDL's CM2 global coupled climate models. Part I: Formulation and simulation characteristics, *J. Clim.*, *19*, 643–674.
Gerdes, R., and C. Köberle (1995), On the influence of DSOW in a numerical model of the North Atlantic general circulation, *J. Phys. Oceanogr.*, *25*, 2624–2641.
Getzlaff, J., C. W. Böning, C. Eden, and A. Biastoch (2005), Signal propagation related to the North Atlantic overturning, *Geophys. Res. Lett.*, *32*, L09602, doi:10.1029/2004GL021002.
Hsieh, W. W., M. K. Davey, and R. C. Wajsowicz (1983), The free Kelvin wave in finite-difference numerical models, *J. Phys. Oceanogr.*, *13*, 1383–1397.
Johnson, H. L., and D. P. Marshall (2002), A theory for the surface Atlantic response to thermohaline variability, *J. Phys. Oceanogr.*, *32*, 1121–1132.
Kawase, M. (1987), Establishment of deep ocean circulation driven by deep-water production, *J. Phys. Oceanogr.*, *17*, 2294–2317.
Knight, J. R., R. J. Allan, C. K. Folland, M. Vellinga, and M. E. Mann (2005), A signature of persistent natural thermohaline circulation cycles in observed climate, *Geophys. Res. Lett.*, *32*, L20708, doi:10.1029/2005GL024233.
Peña-Molino, B., and T. M. Joyce (2008), Variability in the Slope Water and its relation to the Gulf Stream path, *Geophys. Res. Lett.*, *35*, L03606, doi:10.1029/2007GL032183.
Schmittner, A., M. Latif, and B. Schneider (2005), Model projections of the North Atlantic thermohaline circulation for the 21st century assessed by observations, *Geophys. Res. Lett.*, *32*, L23710, doi:10.1029/2005GL024368.
Smethie, W. M. (1992), Tracing the spreading of North Atlantic Deep Water in the western North Atlantic deep western boundary current using the chlorofluorocarbons F-11 and F-12, *Prog. Oceanogr.*, *31*, 51–99.
Smith, R. D., and P. R. Gent (2004), Anisotropic Gent-McWilliams parameterization for ocean models, *J. Phys. Oceanogr.*, *34*, 2541–2564.
Talley, L. D., J. L. Reid, and P. E. Robbins (2003), Data-based meridional overturning streamfunctions for the global ocean, *J. Clim.*, *16*, 3213–3226.
Zhang, R. (2008), Coherent surface-subsurface fingerprint of the Atlantic meridional overturning circulation, *Geophys. Res. Lett.*, *35*, L20705, doi:10.1029/2008GL035463.
Zhang, R., and G. K. Vallis (2007), The role of bottom vortex stretching on the path of the North Atlantic Western Boundary Current and on the Northern Recirculation Gyre, *J. Phys. Oceanogr.*, *27*, 2053–2080.

R. Zhang, GFDL, NOAA, 201 Forrestal Rd., Princeton, NJ 08540, USA. (rong.zhang@noaa.gov)